

EFFECT OF Mn^{3+} SUBSTITUTION ON ELECTRIC AND MAGNETIC PROPERTIES OF $\text{Bi}_{0.8}\text{La}_{0.15}\text{Ho}_{0.05}\text{Fe}_{1-x}\text{Mn}_x\text{O}_3$

S. ANWAR*, J. AHMAD

Department of Physics, Bahauddin Zakariya University, Multan 60800, Pakistan

BiFeO_3 (BFO) is a compound of tremendous interest for researchers for its multiferroic properties above room temperature. A batch of $\text{Bi}_{0.8}\text{La}_{0.15}\text{Ho}_{0.05}\text{Fe}_{1-x}\text{Mn}_x\text{O}_3$ (BLHFMO) was synthesized by solid state reaction method. The structural studies have been carried out by employing X-Ray Diffraction (XRD) and scanning electron microscopy (SEM). The dielectric and magnetic properties have also been investigated by employing relevant techniques. For BLHFMO, with increase in Mn^{3+} concentration structural transition from rhombohedral to orthorhombic phase was detected from XRD results. Moreover high values of dielectric constant in the vicinity of Neel temperature are related to magnetic phase transition. Maximum magnetic response was observed for 10 % manganese concentration.

(Received March 21, 2019; Accepted September 6, 2019)

Keywords: Solid state reaction, Electrical properties, Perovskite, Dielectric Magnetic

1. Introduction

Bismuth ferrite (BiFeO_3) is a potential material for use in practical appliances. This material is fit for applications in sensor devices, memory devices and spintronics due to its fascinating multiferroic properties [1]. It is one of the few materials which show room temperature magnetic and ferroelectric ordering. It has antiferromagnetic Neel temperature (T_N) of 370°C and ferroelectric temperature (T_C) of 810°C [2-3]. However few drawbacks such as high leakage current, high dielectric loss and weak antiferromagnetic character limit its use at room temperature. BFO is already a lone pair multiferroic material, so ion substitution is a common and remarkable effective method to modulate its basic properties and overcome drawbacks. Rare earth (RE) ions (La^{3+} , Ho^{3+} , Er^{3+} etc) substitution at Bi site is expected to distort the cations spacing between the oxygen octahedra and alter the long-range ferroelectric order which can enhance magnetic properties [4-5]. Moreover substitution of La and Ho element can stabilize the perovskite system and is also beneficial for reducing the oxygen vacancies as a result of volatile nature of the Bi element.

Similarly Manganese (Mn) is a particularly interesting element for substitution as it easily changes its oxidation state; furthermore the ionic radii of Fe^{3+} and Mn^{3+} are practically identical with ionic radius approximately equal to 0.645 \AA [6]. However the number of d electrons and effective magnetic moments are different for Fe^{3+} and Mn^{3+} . There are five 3d electrons and an effective magnetic moment of μ_{eff} equal to $5.9 \mu_B$ for Fe^{3+} and four 3d electrons and effective magnetic moment of μ_{eff} equal to $4.9 \mu_B$ for Mn^{3+} . Thus even though Fe^{3+} and Mn^{3+} have equivalent ionic radii the magnetic interaction is affected by the substitution [6-7].

In this work different physical properties for $\text{Bi}_{0.8}\text{La}_{0.15}\text{Ho}_{0.05}\text{Fe}_{1-x}\text{Mn}_x\text{O}_3$ have been measured. Doping was made at B-site to replace Fe^{3+} cations. Different properties as XRD, SEM, dielectric constant, P-E, MH and MT loops were measured to explore the doping effect of Mn in the material. Increased values of dielectric and magnetic properties are obtained for co-doped bismuth ferrite material.

* Corresponding author: sagsgd@gmail.com

2. Experimental

$\text{Bi}_{0.8}\text{La}_{0.15}\text{Ho}_{0.05}\text{Fe}_{1-x}\text{Mn}_x\text{O}_3$ compounds for $x=0.0-0.3$ were prepared by rapid phase sintering solid state reaction (SSR) route. Stoichiometric amounts of precursor materials of better than 99% purity were weighed and grinded using agate mortar and pestle for about 1 h. The above uniform mixture was presintered at 800 °C for 12 h. The presintered powder was pressed into cylindrical pellets of approximately 10 mm diameter and 2 mm of thickness at a pressure of $2.94 \times 10^8 \text{ N/m}^2$ by using a hydraulic press. The final sintering was carried out at 1000°C for 24 h in air atmosphere with a heating rate of 5 °C/min, followed by natural cooling to room temperature. Crystal structure of the samples was determined using x-ray diffraction (XRD) patterns recorded by using a Rigaku diffractometer by employing $\text{Cu-K}\alpha$ radiation. Temperature and field variations of magnetization measurements were carried out using a squid magnetometer in the temperature range of 5–300 K. For the electrical characterizations, electrodes were fabricated by painting silver pastes on both sides of the sample of typical thickness ~ 2 mm. The samples were fired at 150 °C in air for 2 h and furnace cooled to room temperature before carrying out the electrical measurement. The frequency dependent dielectric measurements at several temperatures (30–400 °C) were measured using an LCR meter.

3. Results and discussion

3.1. Structural analysis

Fig. 1 shows the XRD pattern from the sample $\text{Bi}_{0.8}\text{La}_{0.15}\text{Ho}_{0.05}\text{Fe}_{1-x}\text{Mn}_x\text{O}_3$ ($x = 0, 0.05, 0.1, 0.2$ and 0.3). X-ray diffraction (XRD) was used to confirm the pure phase of the material. All major peaks are indexed to different ($h k l$) planes for BiFeO_3 (JCPDS 86-1518). It is found that all the samples are single phase.

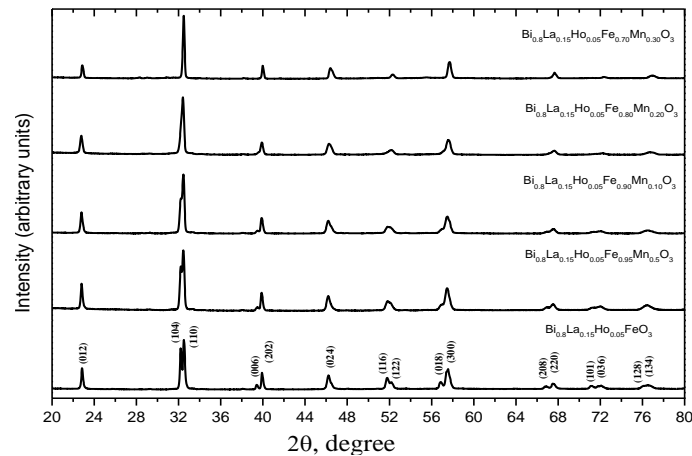


Fig. 1. Powder XRD patterns for $\text{Bi}_{0.8}\text{La}_{0.15}\text{Ho}_{0.05}\text{Fe}_{1-x}\text{Mn}_x\text{O}_3$ ($0.0 \leq x \leq 0.3$).

It is very clear from graph that XRD peak about 32° very clearly splits into two (104) and (110) peaks. Two more observed features are: firstly, peak with (104) hkl value shifted towards larger angle whereas peak with (110) hkl value remained unaffected with increasing Mn substitution from 5% to 30%, secondly, peaks with (104) and (110) hkl values combine to (110) peak in 20% and more Mn doped samples. Also (113) and (006) peaks vanished in 20% Mn substituted sample. These changes suggest lattice deformation in BLHFMO structure which leads a phase change from rhombohedral to orthorhombic in 10% Mn substituted sample. A. Mukherjee *et.al.* [8] and S. Chauhan *et.al.* [9] observed similar type of distortion in Dy and La substituted BFO samples where material faced rhombohedral to orthorhombic structural change. One significant change after doping Mn is the increasing intensity of (110) peak. This indicates that Mn

substitution in place of Fe improves the crystal growth. $\text{Bi}_{0.8}\text{La}_{0.15}\text{Ho}_{0.05}\text{FeO}_3$ is crystallized in rhombohedral structure with space group R3c without any detectable impurity. Grain size calculated by Bragg's formula for considering (110) characteristic peak from XRD pattern is gradually decreased from 140 nm to 93 nm for $\text{Bi}_{0.8}\text{La}_{0.15}\text{Ho}_{0.05}\text{Fe}_{1-x}\text{Mn}_x\text{O}_3$, $x = 0.0$ to 0.2 and for $x = 0.3$ it is 154 nm.

Table 1. Grain size calculated from XRD graphs $\text{Bi}_{0.8}\text{La}_{0.15}\text{Ho}_{0.05}\text{Fe}_{1-x}\text{Mn}_x\text{O}_3$ samples.

Cr concentration (x)	Grain size (nm)
0.00	140
0.05	106
0.10	99
0.20	93
0.30	154

Fig. 2 shows the SEM images for the BLHFMO series sintered at 870-880 °C. Results represent the particle agglomeration during the liquid phase of sintering process. This represents homogenous and dense distribution of particles in nano range.

3.2. Dielectric properties

Dielectric constant (ϵ_r) versus temperature (50-400 °C) graphs for BLHFMO series are shown in Fig. 3. Values are taken between the frequency limits of 50 kHz-640 kHz. Graphs clearly depict that ϵ_r increases at any fixed frequency and temperature for substitution of Mn in BLHFMO samples. Maximum value observed for ϵ_r is 14950 at 50 kHz frequency and 220 °C temperature for $x=0.3$ sample. Dielectric constant value at above mentioned temperature and frequency is 186 for $x=0.0$ composition. So it is confirmed that ϵ_r value changes with temperature and composition. The dielectric constant exhibits a step like increase with increase in temperature. If temperature is fixed then it has highest value at smallest frequency which is decreased with increasing frequency.

Such type of response can be explained according to process of dipole relaxation. For small frequencies ($\sim 50\text{kHz}$), the dipoles have enough time to follow the applied field whereas at large frequencies ($\sim 0.6\text{MHz}$), they are unable to follow the field and undergo relaxation. Graph shown in Fig. 3 exhibits peaks at 394-410 °C for $\text{Bi}_{0.8}\text{La}_{0.15}\text{Ho}_{0.05}\text{FeO}_3$. These temperature versus ϵ_r graphs show peaks shift to higher temperatures with increasing frequency. This type of response is an evidence of existence of the thermally activated relaxation in the material. Similar response is also seen for loss tangent ($\tan\delta$) in the complete temperature range from 50 °C to 400 °C. Its value is found to vary from $\sim 3 \times 10^{-3}$ to ~ 589 at 50 kHz during above temperature range.

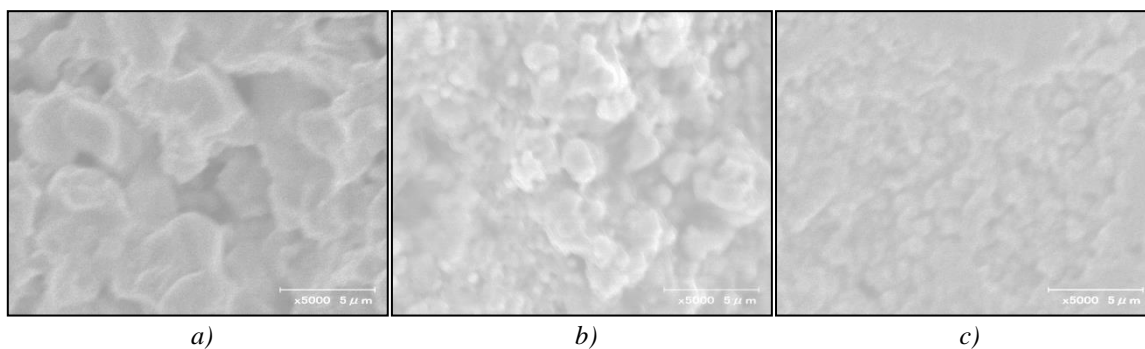


Fig. 2. SEM image for $\text{Bi}_{0.8}\text{La}_{0.15}\text{Ho}_{0.05}\text{Fe}_{1-x}\text{Mn}_x\text{O}_3$ (a) $x=0.0$ (b) $x=0.1$ (c) $x=0.3$.

Increased conductivity in the sample is considered as the reason for increase in loss tangent consistent with the literature [10-12]. Value for ϵ_r don't vary during certain temperature range starting from lower temperature; this temperature gets decreased with increase in Mn doping. Moreover as a result of Mn substitution main dielectric peaks are shifted toward lower temperature and in the end a new transition is observed along with primary dielectric peak for $x=0.4$ concentration. Anjum, Kumar and Yang *et al.* [11, 13-14] observed the similar signature in $\text{BiFe}_{1-x}\text{Mn}_x\text{O}_3$ and $\text{La}_{0.8}\text{Bi}_{0.2}\text{Fe}_{1-x}\text{Mn}_x\text{O}_3$ multiferroic systems. During study of dielectric behaviour for $\text{Bi}_{0.8}\text{La}_{0.15}\text{Ho}_{0.05}\text{Fe}_{1-x}\text{Mn}_x\text{O}_3$ materials, it is found that FE transitions occur at 394 °C, 243 °C, 190 °C and 214 °C for $x = 0, 0.1, 0.2$ and 0.3 samples respectively.

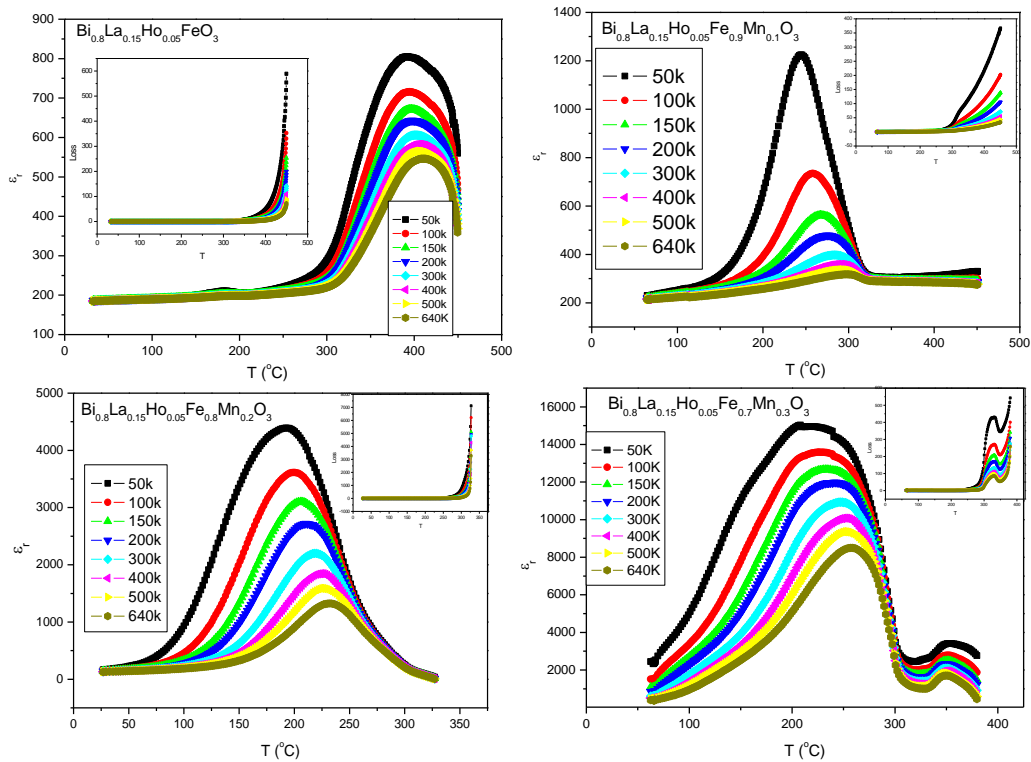


Fig. 3. Dielectric constant as a function of temperature at different frequencies for $\text{Bi}_{0.8}\text{La}_{0.15}\text{Ho}_{0.05}\text{Fe}_{1-x}\text{Mn}_x\text{O}_3$ ($0.0 \leq x \leq 0.3$). Inset shows the $\tan\delta$.

Transition peaks discussed above are well defined even at high frequency of 0.64 MHz. Slight shift in peak position towards higher temperature is observed with change in frequency. If the ferroelectricity in the system is due to Maxwell-Wagner effect, electrode or grain boundary effect; then generally at higher frequencies, transition peaks are not well defined. This also supports the fact that dielectric behaviour is basically due to weak FE nature of these samples.

New peak observed about 350 °C for BLHFMO with $x=0.4$ concentration may be linked with magnetic phase transition. As Neel temperature (T_N) for BFO is about 370 °C, so this irregularity near antiferromagnetic (AFM) Neel temperature shows coupling among magnetic and ferroelectric order parameters. Landau-Devonshire theory of phase transition in magnetically ordered systems explains this dielectric anomaly. According to theory such dielectric anomaly is expected as the effect of diminishing of magnetic order over the electric order [15]. This prominent anomaly can be very clearly observed near magnetic transition temperature in Fig. 3. Significant frequency dispersion at peaks related to T_N is also observed in the graph. At any transition temperature, it moves from lower to higher temperature with increasing frequency. This dispersion accompanies a corresponding decrease in peak value of dielectric constant at T_N resembling ferroelectric relaxor behaviour [16, 17].

Considering dielectric loss (inset of Fig. 3), it shows similar behaviour as like dielectric constant. It also exhibits loss peaks according to the transition curves shown in dielectric constant versus temperature graphs.

Minor shift in peak position with increasing frequency represents relaxor behaviour in materials. In general, at any frequency and temperature, overall increase in dielectric loss is observed for Mn-substituted samples which are considered due to increase in dc conductivity by substitution of Mn in the material.

3.3. Magnetic properties

Fig. 4 presents the change in magnetic moment with reference to temperature (5-300 K) for different samples under both field-cooled (FC) and zero-field-cooled (ZFC) conditions with an applied field of 1000 Oe.

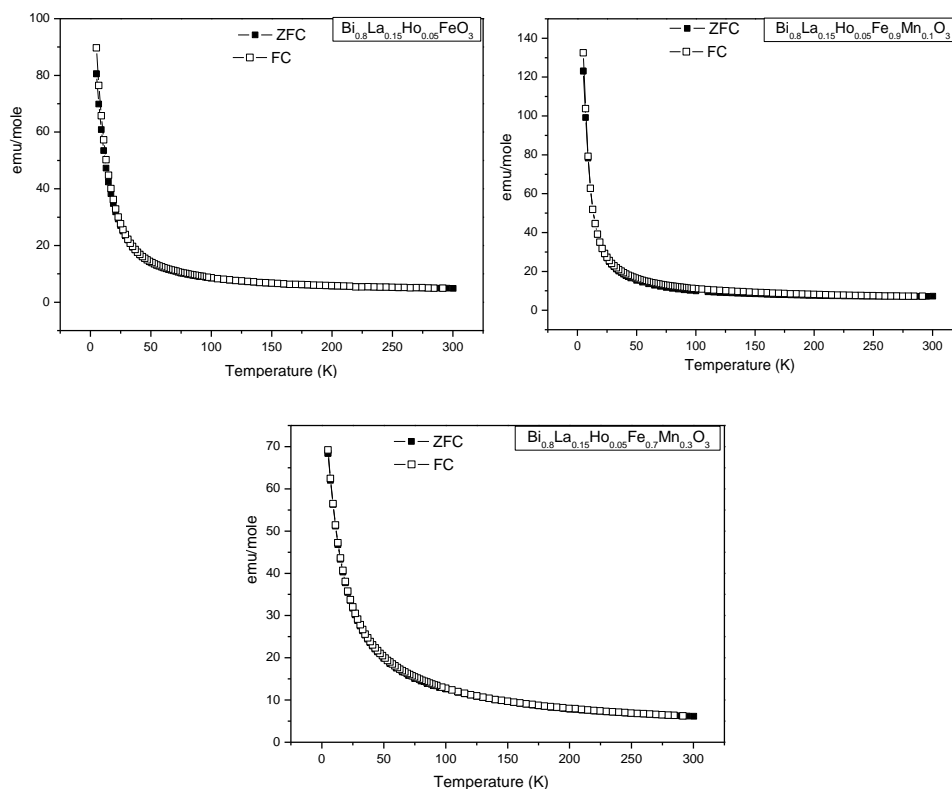


Fig. 4. *M-T* hysteresis loops for $Bi_{0.8}La_{0.15}Ho_{0.05}Fe_{1-x}Mn_xO_3$ ($0.0 \leq x \leq 0.3$).

Table 1 gives the values of magnetization at 5 K for different samples. A significant increase in magnetic moment for the said materials is observed with substitution of Mn. $BiFeO_3$ behaves as an antiferromagnetic material because iron ion's spin is arranged in (111) direction. Possibly, there may be two reasons for the origin and increase in spontaneous magnetization: one, when the size of particles is reduced to about 62 nm then periodicity of the spin cycloid structure can be broken. Second, Mn and Fe have different magnetic moments, so development of local ferrimagnetic spin configuration can be supposed by replacement of iron atoms with manganese at B site [18-19]. The prospective reasons for increase in macroscopic magnetization can be underlying inhomogeneous spin structure, increase in canting angle due to co-doping and creation of Fe^{2+} ions. It is also well known that during high temperature annealing process, coexistence of Fe^{2+} and Fe^{3+} is inevitable [20].

Table 2. Variation of magnetic moment with the concentration of Mn at 5 K.

Mn concentration (x)	Magnetization (FC) at 10 K (emu/mole)
X=0	89
X= 0.1	132
X= 0.3	69

The presence of Fe^{2+} ions may result in double exchange interaction between Fe^{2+} and Fe^{3+} ions via oxygen which can cause enhancement in ferromagnetism [21, 22]. So it can be concluded that increase in Mn concentration enhances magnetization due to charge compensation effect and magnetic moment of Mn itself. However reason of decrease of magnetization in 30% Mn is the structural deformation [8].

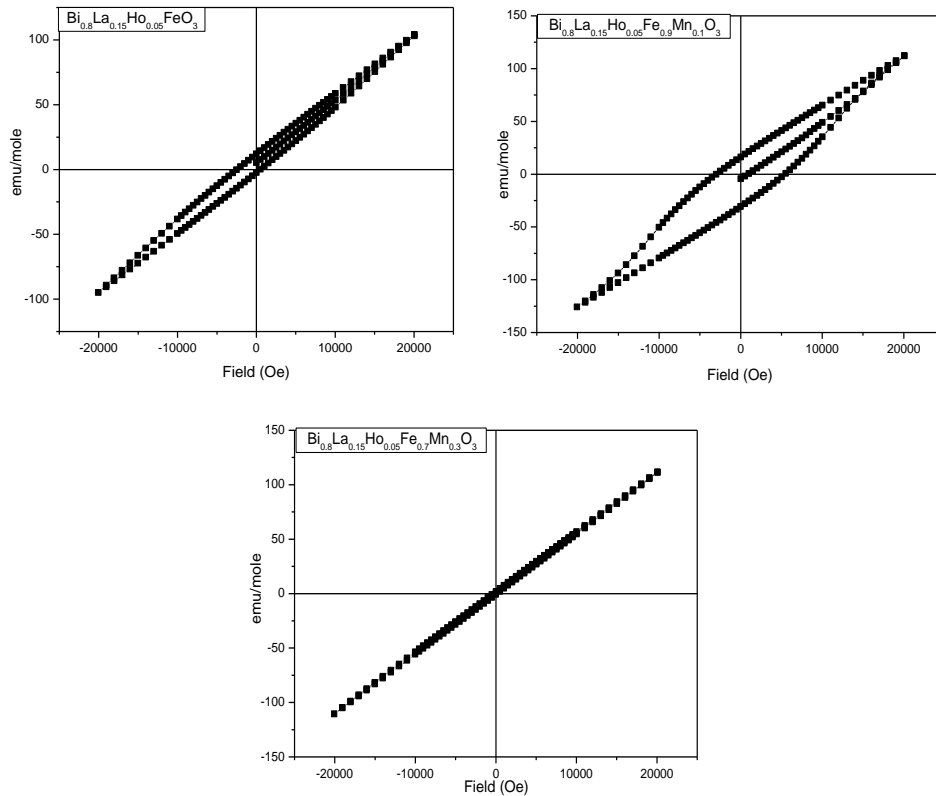


Fig. 5. Room temperature M - H hysteresis loops for $\text{Bi}_{0.8}\text{La}_{0.15}\text{Ho}_{0.05}\text{Fe}_{1-x}\text{Mn}_x\text{O}_3$ ($0.0 \leq x \leq 0.3$).

Magnetisation versus field hysteresis loops shown in Fig. 5 also confirms the same trend. Area of hysteresis loop is increased with initial substitution of Mn up to 10 % which represents increase in magnetic order although loop is not saturated up to field of 20000 Oe (2 T). Coercive field (H_c) value increased from 2.46 KOe to 2.9 KOe for $x = 0$ to $x = 0.1$ sample, respectively. Similarly $2 M_r$ value increased from 15.11 emu/mole to 46.85 emu/mole for increasing concentration from 0 % to 10 % for Mn.

4. Conclusion

Single phase $\text{Bi}_{0.8}\text{La}_{0.15}\text{Ho}_{0.05}\text{Fe}_{1-x}\text{Mn}_x\text{O}_3$ ($x = 0, 0.05, 0.1, 0.2$ and 0.3) samples were prepared by conventional solid state reaction method. Rhombohedral to orthorhombic phase transition was observed for $x \geq 0.2$ samples. Increased value of dielectric constant was obtained with Mn doping in the material. The temperature dependant peaks observed in dielectric response of different samples demonstrate ferroelectric phase transition. Transition temperature is decreased with increasing ratio of Mn contents. Mn substitution also enhanced the magnetisation in the material. Double exchange interaction due to different oxidation states of Fe as a consequence of oxygen vacancies and magnetic moment of Mn are considered the reason behind this enhancement. Structural phase transition is considered as the reason for decrease of magnetisation in $x=0.3$ sample.

References

- [1] Z. X. Cheng, X. L. Wang, K. Ozawa, H. Kimura, *J. Phys. D Appl. Phys.* **40**(3), 703 (2007).
- [2] I. Sosnowska, R. Prezenioslo, P. Fischer, V. A. Murashov, *J. Magn. Magn. Mater.* **160**(1), 384 (1996).
- [3] J.B. Neaton, C. Edrer, U. V. Whgmare, N. A. Splaldin, K. M. Rabe, *Phys. Rev. B* **71**(1), 014113(2005).
- [4] Y. Liu, J. Qi, Y. Zhang, Y. Wang, M. Feng, J. Zhang, M. Wei, J. Yang, *Appl. Surf. Sci.* **427**(A), 745(2018)
- [5] J. Zhu, W. B. Luo, Y. R. Li, *Appl. Surf. Sci.* **255**(5), 3466 (2008).
- [6] R. D. Shannon, *Acta Crystallogr. A* **32**, 751 (1976).
- [7] M. Bakr Mohamed, H. Fuess, *J. Magn. Magn. Mater.* **323**, 2090 (2011)
- [8] A. Mukherjee, M. Banerjee, S. Basu, N. T. K. Thanh, L. A. W. Green, M. Pal, *Physica B*, **448**,199 (2014).
- [9] S. Chauhan, M. Kumar, S. Chhoker, S. C. Katyal, H. Singh, M. Jewariya, K. L. Yadav, *Solid State Commun.* **152**, 525 (2012).
- [10] G. Anjum, S. Mollah, D. K. Shukla, R. Kumar, *Materials Letters* **64**, 2003 (2010).
- [11] G. Anjum, R. Kumar, S. Mollah, D. K. Shukla, S. Kumar, C. G. Lee, *J. Appl. Phys.* **107**, 103916 (2010).
- [12] C. C. Wang, Y. M. Cui, L. W. Zhang, *Appl. Phys. Lett.* **90**, 012904 (2007).
- [13] M. Kumar, K. L. Yadav, *Appl. Phys. Lett.* **91**, 242901 (2007).
- [14] C. H. Yang, T. Y. Koo, Y. H. Jeong, *Solid State Commun.* **134**, 299 (2005).
- [15] W. Eerenstein, N. D. Mathur, J. F. Scott, *Nature* **442**, 759 (2006).
- [16] A. Singh, V. Panday, R. K. Kotnala, D. Panday, *Phys. Rev. Lett.* **101**, 247602 (2008).
- [17] S. Bhattacharjee, V. Panday, R. K. Kotnala, D. Panday, *Appl. Phys. Lett.* **94**, 012906 (2009).
- [18] T.-J. Park, G. C. Papaefthymiou, A. J. Viescas, A. R. Moodenbough, S. S. Wong, *Nano Lett.* **7**, 766 (2007).
- [19] S. Basu, SK. M. Hossain, D. Chakravorty, M. Pal, *Curr. Appl. Phys.* **11**, 976(2011).
- [20] Y. Wang, Q. H. Jiang, H. C. He, C. W. Nan, *Appl. Phys. Lett.* **88**, 142503 (2006).
- [21] J. Wang, A. Scholl, H. Zheng, S. B. Ogale et. al., *Science* **307**, 1203b (2005).
- [22] F. Huang, X. Lu, W. Lin, X. Wu, Y. Kan, J. Zhu, *Appl. Phys. Lett.* **89**, 242914(2006).